eJSE International

Special Issue: Electronic Journal of Structural Engineering 14(1) 2015

Load Testing and In-service Monitoring of Transversely Stressed Deck Unit Bridges

N.S. Ngo, T. Pape & R.P. Kotze

ARRB Group Ltd, Australia

R.W. Pritchard

Queensland Department of Transport and Main Roads, Australia

Email: hanson.ngo@arrb.com.au

ABSTRACT: Transversely stressed precast concrete deck unit bridges are a common type of small and medium span bridge on the Queensland road network. This type of bridge is unique in design featuring transverse post-tensioned stressing bars with a low level of prestressing, stiff upright kerb units and no shear keys. Recent structural assessments of these bridge types has yielded varied and at times inconsistent results, with theoretical structural deficiencies identified at odds with the lack of evidence of structural distress, demonstrating acceptable performance. A test program was developed to address this disparity and improve understanding of the structural performance of these bridge types. This included static and dynamic load testing with various vehicle types, and long-term monitoring of the behaviour of a representative bridge under ambient traffic. The test results have enabled improved understanding of the behaviour and true capacity of this bridge type, as well as providing inputs to enable validation of analytical structural modelling techniques.

Keywords: Load testing, In-service monitoring, Transversely stressed deck unit bridge, Bridge assessment

1 BACKGROUND

The Queensland Department of Transport and Main Roads (TMR) is responsible for the management of a significant number of transversely stressed deck unit bridges on its network. This type of bridge is unique in design featuring transverse post-tensioned stressing bars with a low level of prestressing, stiff upright kerb units and no shear keys.

The most common analytical method to assess this type of bridge is based on a grillage analogy (Hambly 1991), which models the bridge as a grid of longitudinal and transverse beams. A number of other methods are also available, such as the theory of orthotropic plates (Hulsbos 1962), finite strip (Buckle 1984), and finite element methods (Fu et al. 2011). While the sectional properties and stiffness of the longitudinal members are straightforward to determine, differences in opinion currently exist regarding the appropriate modelling of transverse members. West (1973) and El-Remaily (1996) implemented a simple grillage model, in which the stiffness of longitudinal and transverse members was calculated based on the full cross section. This method, however, did not take into account the effects of transverse stressing bars or the behaviour of the interface between adjacent deck units. Hambly (1991) used pin connections between longitudinal members for bridges without shear keys, accounting for shear transfer only. Buckle (1984) assumed negligible transverse bending stiffness and near-rigid stiffness for shear, axial and torsional actions. Hulsbos (1962) established stiffness ratios between transverse and longitudinal members for use in the simple grillage models, however these ratios were dependent on various factors such as the position and magnitude of the load and the transverse post-tensioning force applied. Badwan and Liang (2007) implemented the Hambly (1991) method using equivalent transverse members in grillage analysis, however this method is only applicable for structures with shear keys. Recently, Fu et al. (2011) used the finite element method to model the interface shear friction between adjacent deck units. While this method can address the level of transverse post-tensioning and shear-transfer strength of the bridge deck, it is resource-intensive and thus uneconomical for a routine assessment of deck unit bridges.

The latest TMR assessment method for deck unit bridges (TMR 2013) mostly incorporates relevant procedures from the abovementioned methodologies; however inconsistencies have been identified between the assessment models and the actual condition and performance of the structure. In particular, previous models have identified cases of overloading, specifically in the stiff kerb units. In contrast, the majority of in-service deck unit bridges across the TMR network shows no external/visual evidence of structural distress, which disagrees with theoretical predictions.

Based on these disparities and the lack of confidence in modelling accuracy of this bridge type, a research program has been developed. The goal of this program is to improve assessment techniques and modelling of deck unit bridges in the prediction of actual performance under live load. The three-year program involves load testing and long-term monitoring of a representative in-service deck unit bridge, shear and bending moment capacity load testing on individual deck units, and full-scale destructive load testing of a simulated deck unit bridge. This paper reports on the outcomes of the first year of the test program.

Canal Creek Bridge which is located on the Finders Highway between Julia Creek and Cloncurry, Queensland was selected for investigation based on poor assessment results and being representative of a family of short-span deck unit bridges on a key freight route subject to some vehicle permit restrictions. The load tests and in-service monitoring were undertaken over a two week period in May 2014. The results of these tests will be used to review and improve bridge assessment methodologies for these bridge types, which may ultimately lead to the relaxation of conservative restrictions on existing bridges on key routes, increasing freight movement, productivity and economic benefits.

2 TEST PARAMETERS

2.1 Test bridge

Canal Creek Bridge is generally in good condition with no evidence of structural cracking or spalling. This is inconsistent with deficient structural assessment results as discussed above, which has been the predominant factor motivating the current investigation.

The bridge, designed in 1970 for H20-S16 loading, is located in a dry, arid environment, traversing a predominantly dry river bed. It comprises two-simply-supported symmetrical 8.3 m long precast prestressed concrete deck unit spans with a two-lane carriageway (6.7 m width). Each span consists of 11 internal deck units (rectangular hollow section) and two upright external kerb units (rectangular solid section). The precast units are placed side-by-side, with a 25 mm mortar layer between units, and transversely post-tensioned with four, equally spaced, bonded Macalloy bars (

Figure **1**). Approximately 400 vehicles per day cross the bridge, including 30% heavy vehicles.

The substructure consists of two abutments and a central pier, each comprising a cast-in situ concrete headstock supported on four precast concrete piles. A 100 mm asphalt layer with 1.5% crossfall from the centreline covers the deck units. The road surface is in relatively good condition, with the exception of a depression in the transition zone behind each abutment, resulting in a ‘jump’ onto the bridge deck. An undulating road profile also exists on the Julia Creek approach.

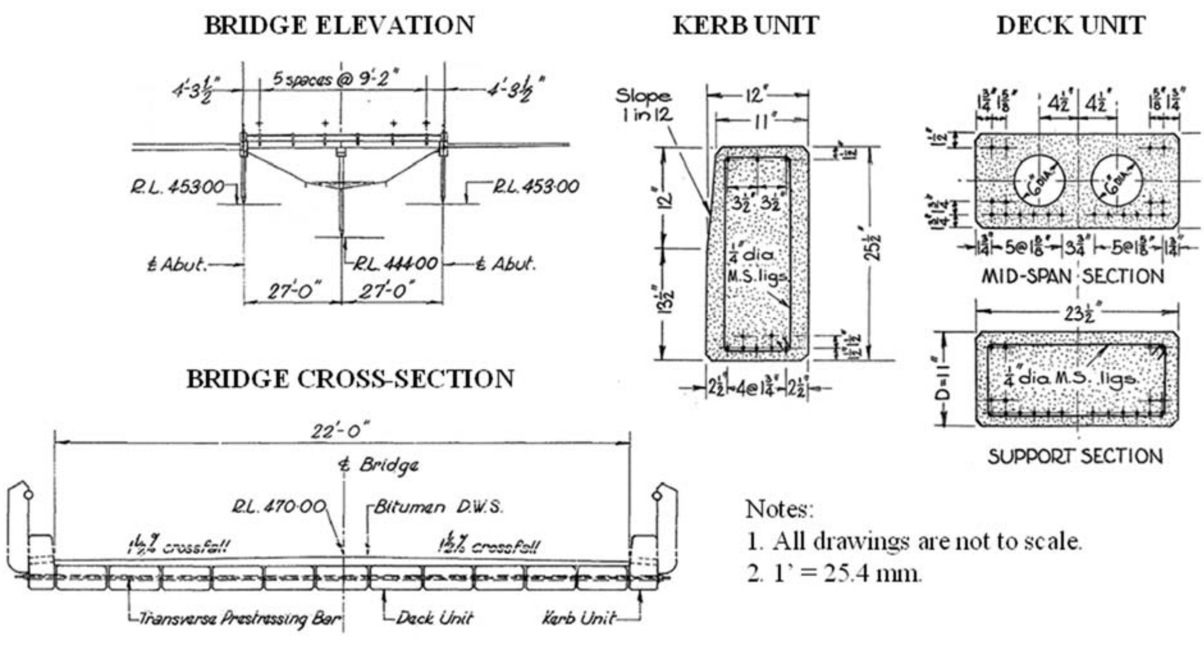

Figure 1. Canal Creek Bridge

2.2 Test vehicles

Four test vehicles were selected for the controlled load test (
Figure **2**), including a 4-axle 48 t all-terrain hydro-pneumatic crane (CR), an articulated, steel suspension, general mass limit (GML) semi-trailer (ST1), an articulated, air-bag suspension, high mass limit semi-trailer (ST2), and a steel-leaf suspension GML road train with two trailers (RT).

2.3 Bridge instrumentation

Table 1 presents the data capture requirements for the bridge with the resulted instrument plan shown in
Figure **3**. Most of the instrumentation was installed on span 1, with the installation of one LVDT and one strain gauge included with span 2 to compare the performance between the two spans.

3 IMPACT MODAL ANALYSIS

Prior to conducting the load tests, a modal analysis was conducted on the superstructure of span 1 to determine the dynamic and stiffness characteristics of the bridge. This involved impacting the soffit of the deck with an instrumented 6 kg specialist hammer at preselected locations and recording the dynamic response from the installed accelerometers. Fundamental frequencies and damping characteristics of the bridge were subsequently determined, as well as the deflected shape of the bridge at each fundamental frequency.

Results from the impact modal analysis indicate that the bridge was relatively stiff, with the first fundamental frequency recorded at 12.3Hz and a corresponding 4% damping. All modal results are summarised in Table 2.

4 STATIC AND DYNAMIC LOAD TESTS

The test program included both static and dynamic testing, and required each test vehicle to travel across the bridge at speeds increasing incrementally from crawling speed (approximately 5 km/h) to 110 km/h at various transverse deck locations and in both directions (to Julia Creek and Cloncurry). Additional static load tests were conducted with both semi-trailers crawling across the bridge simultaneously in both directions. In total, 90 individual vehicle runs were recorded.

Theoretical grillage models were used to determine the likelihood of tensile cracking occurring during the testing. Strain limits for live load were determined based on the design tensile stress limit (AS 5100.5: 2004), which were 248 $\mu\varepsilon$ and 410 $\mu\varepsilon$ for the kerb and deck units respectively. During test runs, peak strain results were reviewed against the calculated limits, with tests proceeding provided these limits were not exceeded.

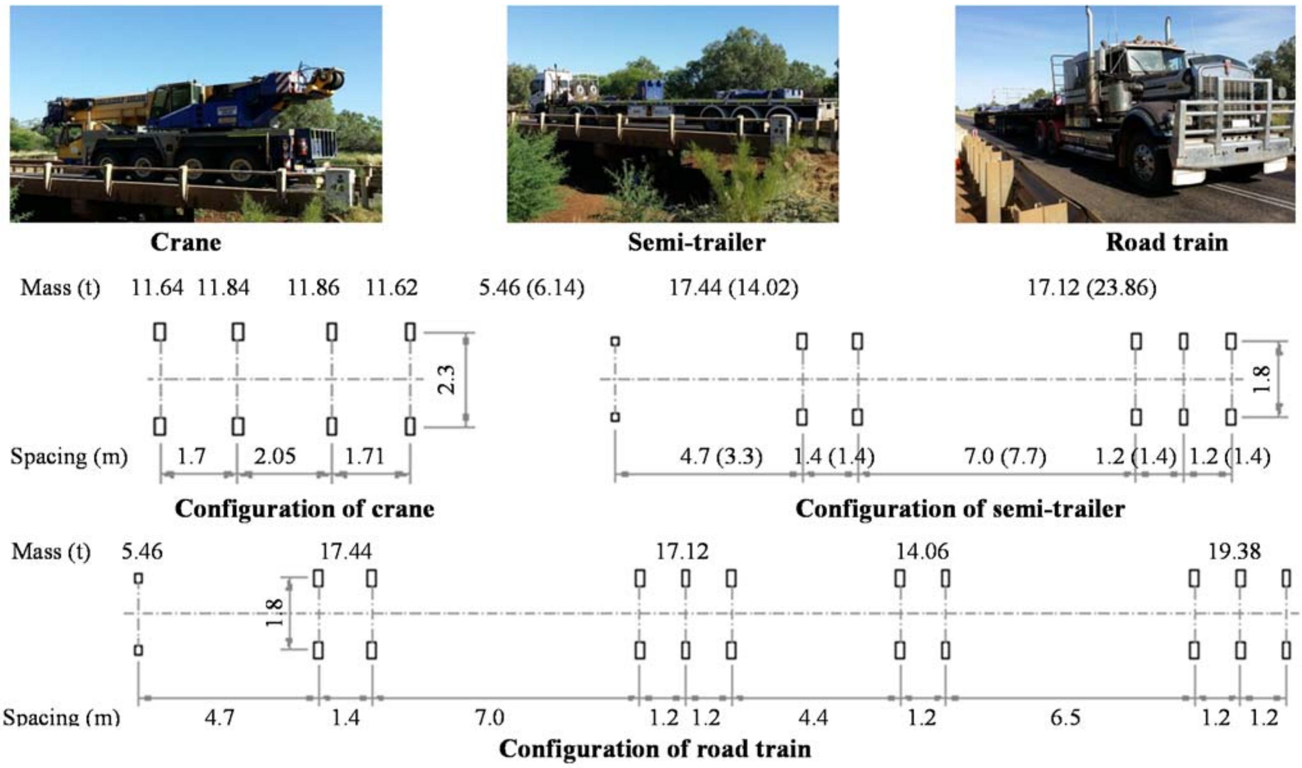

Note: the numbers in parenthesis () are used for the semi-trailer 2 (air-suspension).

Figure 2: Test vehicles

Table 1. Data capture requirements for Canal Creek Bridge load test

What	Where	Instrument used
Deflections	• Midspan of every deck unit (Span 1) • Quarter span for deck units DU1, DU3, DU5 and DU7 (Span 1) • Either ends of the centre deck unit DU7 (Span 1) • Midspan of DU7 (Span 2)	Linear variable displacement transducers (LVDT1–LVDT24)
Bending strains	• Midspan of every deck unit (Span 1) • Top and side face of the kerb DU1 (at Midspan, Span 1) • Midspan of DU7 (Span 2)	Foil strain gauges (SG1–SG15)
Dynamic response of deck	• Midspan and either end of DU7 (Span 1) • Headstock of Abutment 1and Pier 1)	Accelerometers (3D on pier and abutment headstock) (A1–A9)
Gap opening between deck units	• Midspan, between deck units DU1–DU7 (Span 1)	Proximity probes (PS1–PS6)
Rotation of deck units	• Midspan, at soffit of deck units DU1–DU7 (Span 1)	Tilt meters (TM1–TM7)

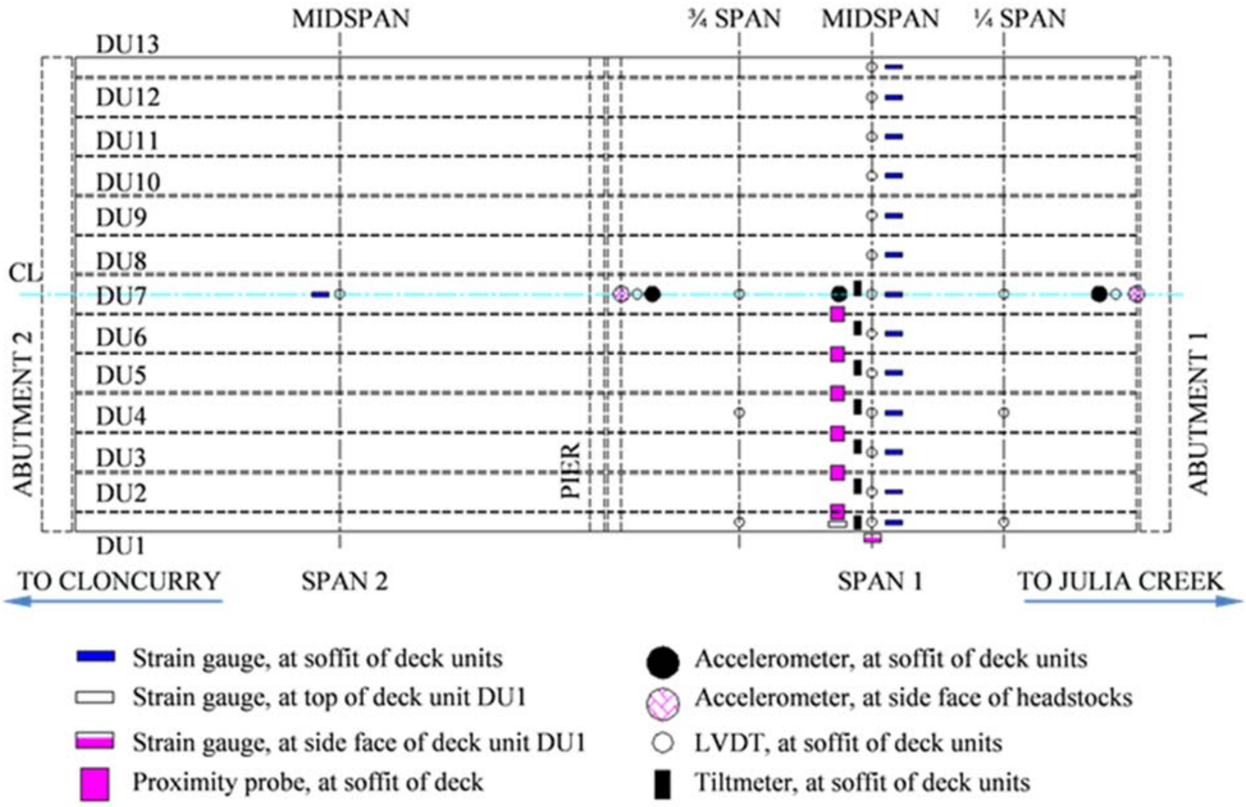

Figure 3. Instrumentation plan

Table 2. Measured frequencies

Fre-quency	Damping ratio (%)	Description
12.3	4.0	Similar to fundamental bending
14.6	6.5	Fundamental bending
19.2	4.8	Fundamental torsion
29.0	3.4	Higher order torsion

4.1 Strain and deflection waveforms

Figure **4** and Figure **5** show representative waveforms of strains and deflections respectively for the test crane travelling towards Cloncurry at crawling speed and 60 km/h for selected deck units. The following generic observations are made:

– Localised effects were observed for the deck units under direct contact with a wheel line (for example, as shown for SG3 and SG7 in
– Figure **4**). Other deck units that were not under direct contact with a wheel line perform very similar to part of a solid deck.
– Some degree of load continuity between the spans over the pier were observed, despite the fact that the spans are simply-supported.
– Increases in vehicle speed mostly resulted in an increase in peak strains and deflections.

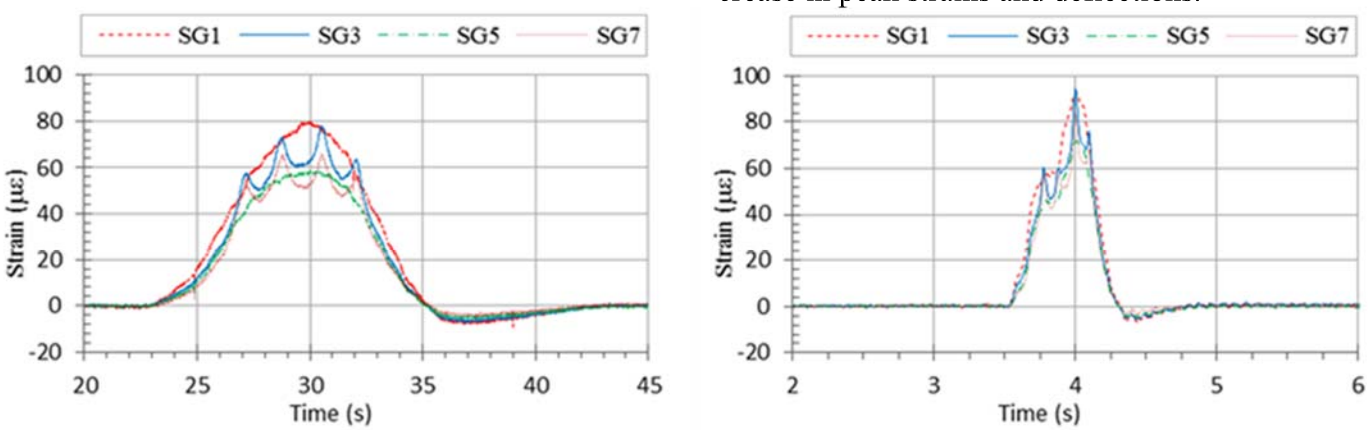

a) At crawling speed

b) At 60 km/h

Figure 4. Representative waveforms of strains (crane travelled to Cloncurry)

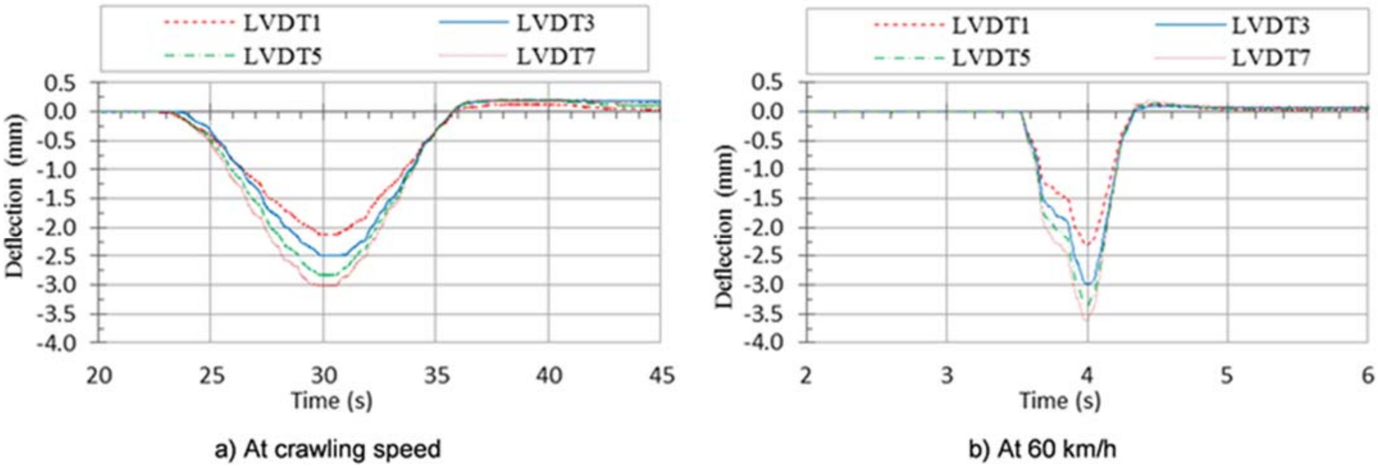

Figure 5. Representative waveforms of deflections (crane travelled to Cloncurry)

4.2 Transverse distribution of midspan deflections and strains

For crawling tests, each test vehicle crossed the bridge at three transverse locations (bridge centreline, 0.6 m and 0.3 m from kerb) in both directions.

Figure 6 presents the distribution of static deflections of the deck units at midspan under the test crane in these crawling tests.

Preliminary calculations based on measured deflections and bending stiffness show that a kerb unit carries a maximum of 39% of the crane load and an individual deck unit carries a maximum of 8%. This agrees with the theory that the kerb unit attracts a large portion of the load due to its significantly higher stiffness. Slightly different distributions were obtained for other test vehicles, however the kerb unit still attracts a significantly higher portion of load than any individual deck unit. The derived transverse distribution based on measured deflection data agrees well with Roesli et al. (1956).

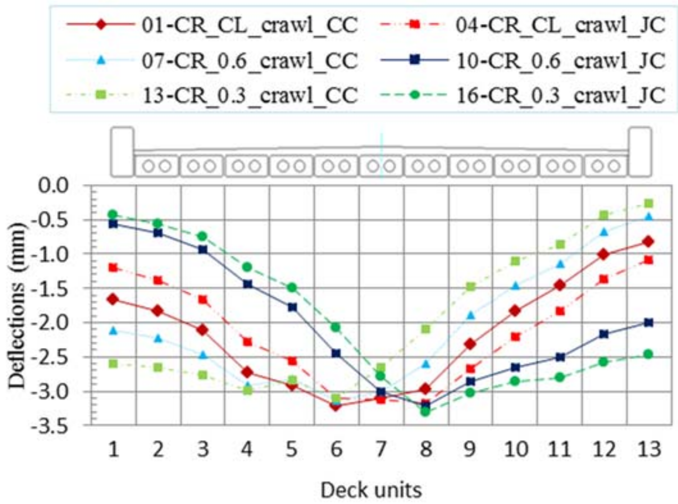

Figure 6. Transverse distribution of the midspan deflections

Similarly,

Figure 7 presents the distribution of static tensile bending strains at the midspan section of the deck units under the test crane at various transverse locations in both travel directions. As expected the peak strains occurred on the kerb unit when the crane was closest to the kerb.

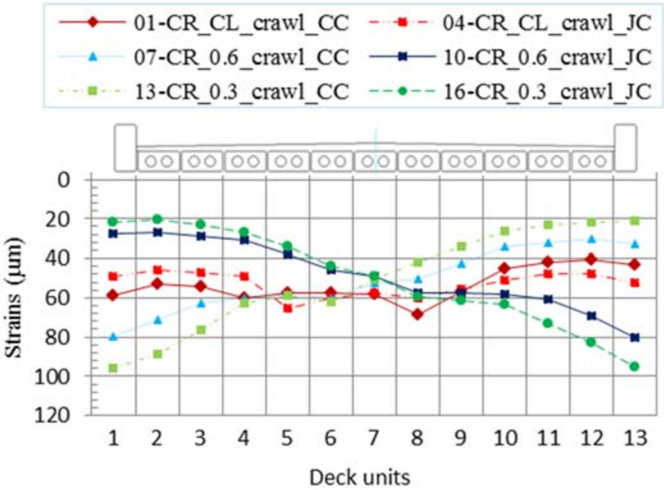

Figure 7. Transverse distribution of the midspan strains

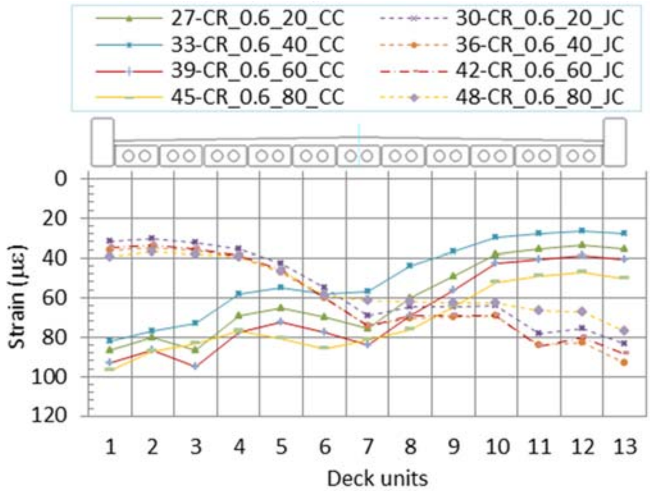

Figure 9. Dynamic strains at the midspan sections

4.3 Envelope of peak midspan deflections and strains

Test results generally showed that the crane induced the highest load effects of all test vehicles. The maximum static deflections recorded were 2.1 mm and 3.3 mm for a kerb and deck unit respectively under the crane for lane and centreline runs. Peak static strains were 96 με and 93 με respectively.

Figure 8 and

Figure 9 show that an increase in speed caused minimal increase in dynamic strains or deflections for the kerb units. Increased dynamic effects were observed in other tests, and are discussed in more detail in Section 0. For all cases, the measured peak strains were significantly lower than the tensile cracked strain limits. This supports the observation that the superstructure is in good condition and free of cracks.

Peak compressive strains at the top of kerb unit DU1 were recorded with the maximum value of 162 με where the crane was closest to the kerb.

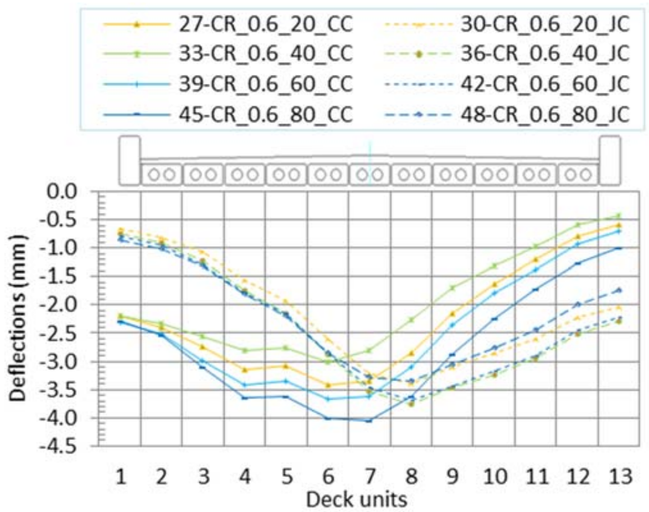

Figure 8. Dynamic deflections at the midspan sections

4.4 Relative movements between the deck units

Figure **10** and Figure 11 show typical waveforms recorded for the rotations and gap openings respectively between instrumented deck units. A maximum rotation of 108 milli-degrees was measured on DU6 for the crane travelled at 10 km/h, and a maximum gap opening of 177 µm was measured between DU6 and DU7 for the crane travelled at 80 km/h. The gap opening returned to zero once loading is removed.

A preliminary analysis showed that while the deck unit rotations were evenly distributed and appeared to coincide with the slopes of the transverse deflection curve as observed by Roesli (1956), there are pronounced localised effects related to the opening of the gap between the deck units that are under direct contact with wheel loads. As such, the relative vertical movement of the deck units was minimal and there was reversible opening in the mortar gap between the deck units. The mechanism of how relative movements between deck units affect the transfer of transverse load requires further analysis.

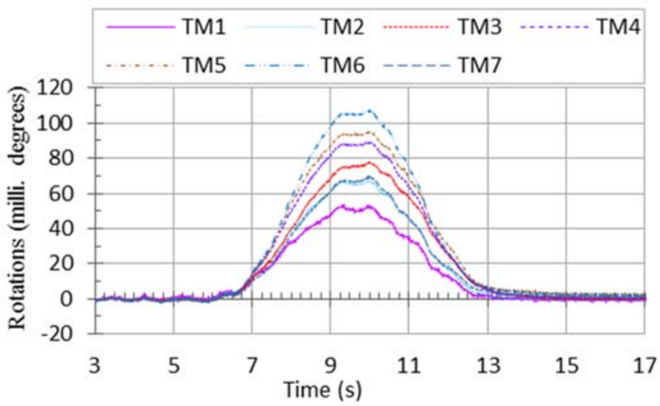

Figure 10. Example waveform of deck unit rotations, crane, 0.6 m, 10 km/h, to Julia Creek

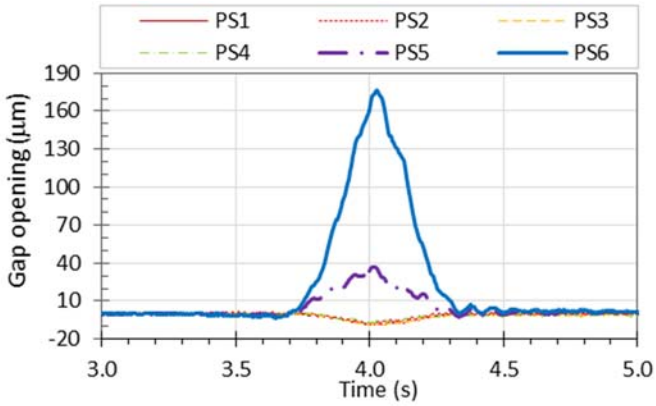

Figure 11. Example waveform of gap openings between deck units, crane, 0.6 m, 10 km/h, to Julia Creek

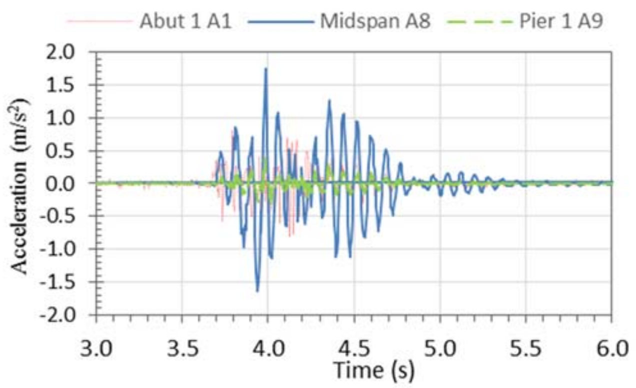

Figure 12. Span 1 acceleration response (crane travelled to Cloncurry at 80 km/h)

4.5 Dynamic response

Accelerometer data was also captured, providing an indication of the dynamic response of the superstructure and substructure under live load. Data for a representative case (the test crane travelling at 80 km/h) is presented and discussed in the following sections.

4.5.1 Superstructure accelerations

Figure **12** presents the waveforms of three accelerometers installed at the midspan and support sections of the central deck unit DU7. As expected, the midspan accelerations were more sensitive to load and were significantly larger than those adjacent to the supports, with almost twice the magnitude recorded in some cases. The dynamic response of the section adjacent to the abutment was also greater than those recorded adjacent to the pier.

Data recorded on these accelerometers under other vehicles show that the passage of the crane and the second trailer of the road train elicited a greater dynamic response compared to those recorded for the two semi-trailers.

4.5.2 Substructure accelerations

The dynamic responses of Abutment 1 and Pier 1 headstocks were measured in three directions: vertical, longitudinal (along the length of the bridge) and transverse (perpendicular to the bridge centreline). Representative waveforms are shown in
Figure **13** and
Figure **14**, respectively, for the crane travelling at 80 km/h to Cloncurry. Generally, the vertical dynamic response between the pier and abutment were comparable for various speeds and vehicles. Dynamic responses were more pronounced particularly for the steel suspension semi-trailer (ST1) at various speeds over the abutment rather than the pier, which may be in response to the poor road profile behind the abutment.

The vertical accelerations measured in the abutment headstock was greater than those measured in the longitudinal and transverse directions. Conversely, accelerations measured in the longitudinal direction for the headstock were greater in magnitude than in other directions. This trend was more pronounced with increasing vehicle speed and the frequency response to live loading. This may be indicative of the continuity effects in the superstructure over the pier.

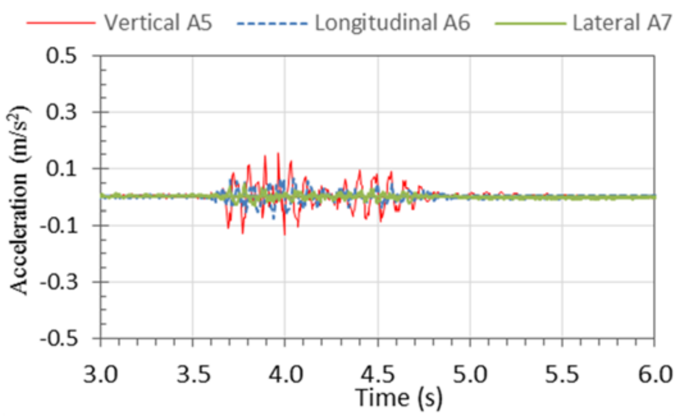

Figure 13. Dynamic response of abutment A1 (crane travelled to Cloncurry at 80 km/h)

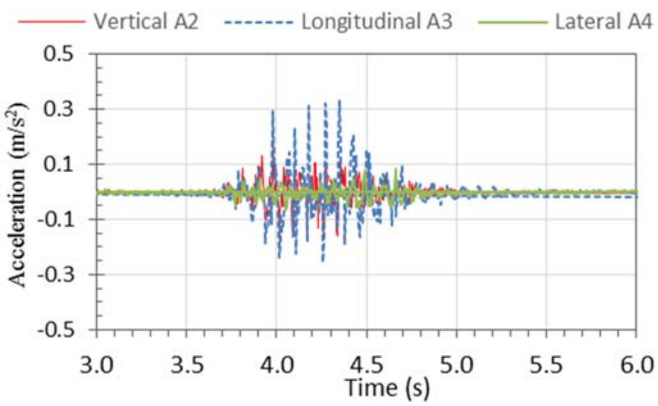

Figure 14. Dynamic response of the pier (crane travelled to Cloncurry at 80 km/h)

4.6 Dynamic increments

The dynamic increment (DI) was calculated for each test vehicles at various speeds based on the following equation:

$$DI = \frac{\varepsilon_{dynamic} - \varepsilon_{static}}{\varepsilon_{static}} 100[\%] \qquad (1)$$

where $\varepsilon_{dynamic}$ is the peak dynamic strain in relation to live load at each speed and ε_{static} is the static strain measured at the corresponding live load position.

The representative DI was obtained by considering peak strains achieved in the deck units directly affected by live load for the corresponding direction of travel. From these values, the maximum peak and average peak DI values were obtained, and taken to be the representative DI values for the superstructure for each vehicle for each speed variation and direction of travel. Peak and average DI values for each vehicle are summarised in **Error! Reference source not found.**. The average DI values are graphically illustrated in

Figure **15**, with positive speed values indicative of travel towards Julia Creek, and negative values towards Cloncurry.

The patterns between peak and average DI values are relatively similar. On average, peak DI values were consistently less than 30%, with the exception of one outlier of 82% recorded for ST1 travelling towards Julia Creek. This value is not considered to be a true representation of the bridge. The majority of peak DI values were determined for vehicles travelling towards Cloncurry, of which the overall peak was 48% for the semi-trailer ST1.

Table 3. Peak and average DI values for each vehicle type

Test vehicle	Peak		Average	
	To Julia Creek	To Cloncurry	To Julia Creek	To Cloncurry
Crane (CR)	16% (80 km/h)	38% (80 km/h)	13% (80 km/h)	24% (80 km/h)
ST1	82% (100 km/h)	48% (80 km/h)	53% (100 km/h)	23% (40 km/h)
ST2	8% (80 km/h)	37% (100 km/h)	1% (80 km/h)	26% (100 km/h)
Road train (RT)	24% (100 km/h)	24% (40 km/h)	14% (20 km/h)	19% (40 km/h)
Overall Maximum	82%1	48%	53%1	26%

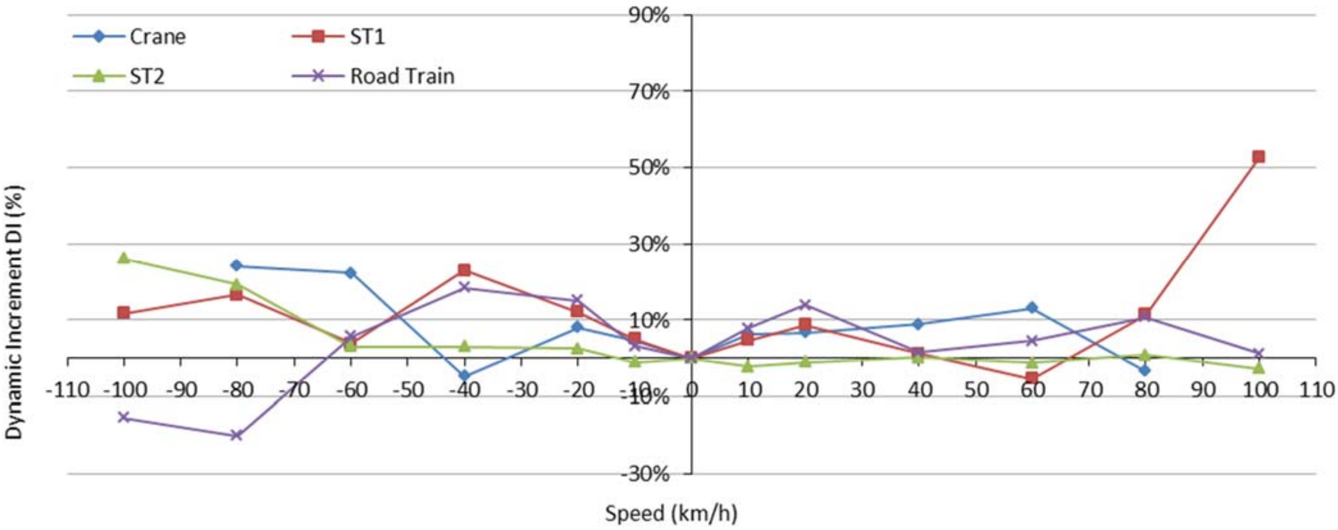

Figure 15. Average dynamic increments

Higher DI values were generally recorded for vehicles travelling to Cloncurry with increasing speed, with the exception of the peak outlier for ST1. Semi-trailer ST2 induced the lowest dynamic response of all vehicles, followed by the crane, with DI values generally less than 20%, with the exception of speeds exceeding 40 km/h and 60 km/h for crane and ST2 respectively, where DI values approached 40%.The increasing dynamic response to speed and direction of travel may be indicative of frequency matching between the suspension systems of the vehicles and the bridge, coupled with the road profile at this location.

Negative DI values were recorded for the road train which are not considered critical in the dynamic response of the bridge, but may be indicative of out-of-phase body bounce, where dynamic wheel forces are low when the vehicle is near midspan.

5 IN-SERVICE MONITORING

In-service monitoring was undertaken to capture unrestricted traffic data and effects under normal conditions. In particular, there was interest in determining whether the selection of test vehicles were representative of typical/normal traffic on the route and whether the bridge was at risk of overloading.

Information regarding the number of heavy vehicle events recorded during the monitoring period is summarised in Table 4. This is based on strain data collected for deck unit DU6 (the gauge most likely under a wheel line of random traffic). A total of 1413 events were recorded, with 562 having measured strains greater than 10 με.

Scatter plots for deflections and strains captured at mid-span during in-service monitoring are presented in

Figure **16** and

Figure **17** for deflections and strains of deck unit DU7 respectively. The maximum effects induced by the test crane are included as reference. The predominant number of traffic events registered strains less than 20 με, and peak values recorded were similar to those obtained in the controlled tests. Based on the data collected, there currently appears to be a low risk of excessively large, heavy vehicle events crossing the bridge, resulting in overloading.

Only a small number of recorded events induced large deflections and strains comparable to the peak values induced by the test crane from the controlled load tests. The corresponding strains and deflections recorded for a peak event was 95 με and 2.4 mm for a kerb unit (DU1) and 89 με and 4.5 mm for a deck unit (DU7) respectively.

6 CONCLUSION

The Canal Creek Bridge east of Cloncurry has been successfully instrumented and tested for various vehicle types. The load test forms part of a research program to investigate inconsistencies between predictive analytical models and observed performance and condition of a deck unit bridge type. Initial results show that the bridge performed better than theoretical model predictions. Live load distribution is similar to that of a flat slab, and as predicted, the kerb units attract the majority of load. The results also indicate that the dynamic response of the bridge was lower for the hydro-pneumatic crane and air-bag suspension semi-trailer at lower speeds, and greater for the semi-trailer with steel-leaf suspension. The condition of the road approaches exacerbated dynamic effects. Preliminary indications are that the substructure yielded a reduced dynamic response in comparison to the superstructure. In-service monitoring data highlighted that peak values were similar to those recorded for the test vehicles and that overloading on this route presents a relatively low risk to the bridge. The results will enable TMR to review the bridge assessment methodology to improve confidence and ensure a realistic approach in modelling deck unit bridges across their network.

Table 4. Recorded number of heavy vehicle crossing events

Logging period	Total number of extracted events	Number of events greater than 5 με	Number of events greater than 10 με
Friday, 2 May 20141	211	167	78
Saturday, 3 May 2014	236	183	86
Sunday, 4 May 2014	265	219	97
Monday, 5 May 2014	287	248	120
Tuesday, 6 May 2014	358	294	150
Wednesday 7 May 20142	56	42	31
Total	1413	1153	562

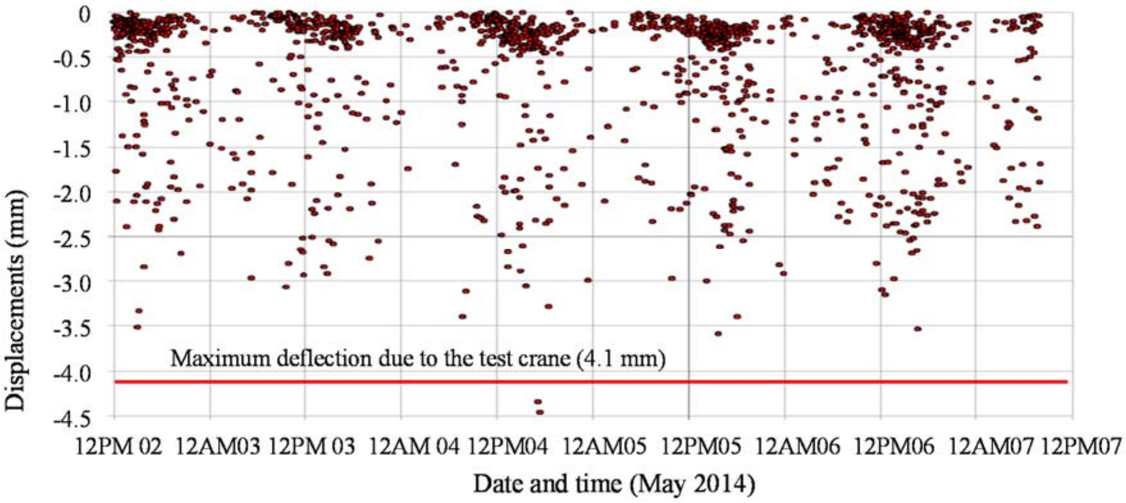

Figure 16. Scatter plot for the midspan deflection of deck unit DU7

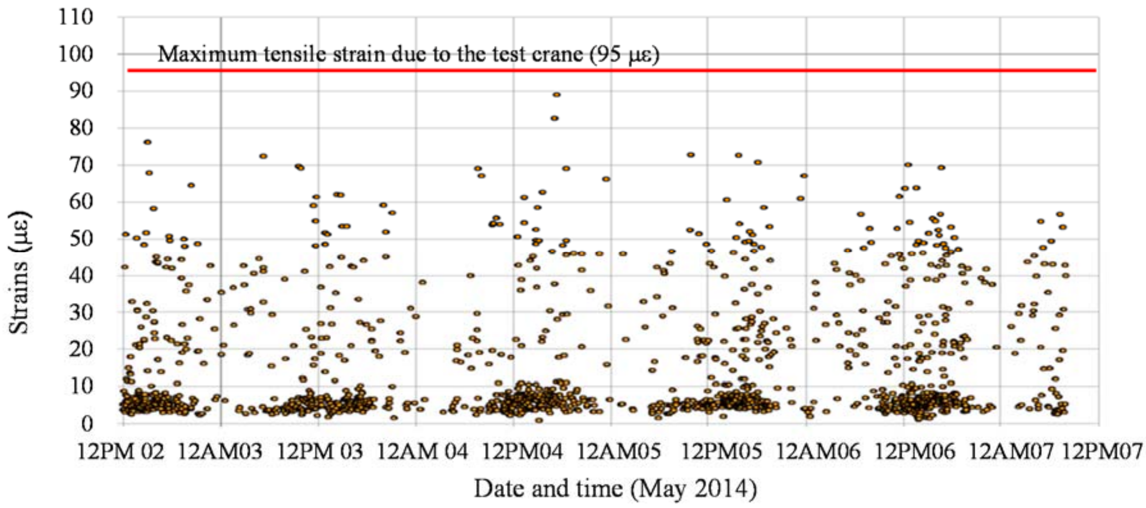

Figure 17. Scatter plot for the midspan strain of deck unit DU7

7 REFERENCES

Badwan, I., and Liang, R.Y., "Transverse post-tensioning design of precast concrete multibeam deck", *PCI Journal*, Vol. 52, No. 4, 2007, pp 84-92.

Buckle, I.G., "Methods of analysis of multi-beam bridges", *Road Research Unit Bulletin*, No. 72, 1984, National Roads Board, Wellington, New Zealand.

El-Remaily, A., Tadros, M.K., Yamane, T., and Krause, G., "Transverse design of adjacent precast prestressed concrete box girder bridges", *PCI Journal*, Vol. 41, No. 4, 1996, pp. 96-113.

Fu, CC., Pan, Z., and Ahmed, M.S., "Transverse posttensioning design of adjacent precast solid multibeam bridges", *Journal of Performance of Constructed Facilities*, Vol. 25, No. 3, 2011, pp. 223-30.

Hambly, E.C., 1991, *Bridge deck behaviour*, 2nd edn, CRC Press, Boca Ranton, Florida, USA.

Hulsbos, C.L., "Lateral distribution of load in multibeam bridges", *Highway Research Board Bulletin*, No. 339, 1962, pp. 67-79.

Roesli, A., Smislova, A., Ekberg Jr, C.E., and Eney, W.J., "Field test on a prestressed concrete multi-beam bridge", *condensed version given by C.E. Ekberg, Jr. at the Annual Meeting of Highway Research Board, Jan. 20, 1956*, Fritz Laboratory Reports, Paper 1545.

TMR 2013, *Tier 1 bridge heavy load assessment: criteria*, V3.10, Queensland Department of Transport and Main Roads, Brisbane, Qld.

West, R., "Recommendations on the use of grillage analysis for slab and pseudo-slab bridge decks", 1973, Cement and Concrete Association & Construction Industry Research and Information Association, London, UK.

Australian Standards AS 5100.5-2004, Bridge design: concrete.

8 ACKNOWLEGDEMENTS

The authors wish to thank the TMR Deputy Chief Engineer (Structures), Dr. Ross Pritchard, for his permission to publish this paper and acknowledge the contribution provided by other staff from the TMR E&T. The views expressed in this paper are those of the authors and do not necessarily reflect the views of TMR. We also would like to acknowledge the contribution by SLR Consulting for providing bridge instrumentation and data acquisition services.